

LISA: A Layer-wise Integration and Suppression Approach for Hallucination Mitigation in Multimodal Large Language Models

Zhihui Guo¹, Xin Man¹, Hui Xu¹, Jie Shao^{1,2} Zhiguo Jiang³, Xianchao Zhang³, Heng Tao Shen²

¹Shenzhen Institute for Advanced Study, University of Electronic Science and Technology of China

²Sichuan Artificial Intelligence Research Institute, Yibin

³Provincial Key Laboratory of Multimodal Perceiving and Intelligent Systems, Jiaxing University

{zhihuigu,manxin}@std.uestc.edu.cn, {huixu.kim,shaojie}@uestc.edu.cn, xidianzhiguo@163.com, zhangxianchao@zjxu.edu.cn, shenhengtao@hotmail.com

Abstract

Multimodal Large Language Models (MLLMs) excel in vision-language tasks such as image captioning but remain prone to object hallucinations, where they describe objects that do not appear in the image. To mitigate this, we propose **LISA**, a Layer-wise Integration and Suppression Approach. LISA leverages the layer-wise functional roles in MLLMs: shallow layers provide visual grounding, middle layers encode semantics, and deep layers tend to amplify spurious signals. First, layer-wise spectral modulation stabilizes attention by suppressing over-amplified activations in deeper layers while preserving alignment cues in earlier layers. Second, token-level logits from selected layers are fused via anchor-based routing, with token-wise anchor selection and soft logit fusion enabling adaptive integration during decoding. LISA is fully **plug-and-play** and can be seamlessly integrated into existing MLLMs, including Qwen2.5-VL. Experiments on multiple benchmarks show that LISA reduces hallucinations by up to 53.6% in CHAIR_I and improves POPE F1 by up to 5.1%, demonstrating strong generalization across models and tasks. Our code is available at <https://github.com/zhlisa1010-eng/LISA>.

Introduction

The rapid progress of Large Language Models (LLMs) (Floridi and Chiratti 2020; Touvron et al. 2023; OpenAI 2023; Ru et al. 2025) has fostered Multimodal Large Language Models (MLLMs) (Liu et al. 2024b; Dai et al. 2023; Bai et al. 2023), which unify vision-language tasks such as image captioning and visual question answering. Despite these advancements, a persistent issue remains: MLLMs frequently exhibit **object hallucination** (Rohrbach et al. 2018; Zhang et al. 2025b), a specific type of hallucination where the model describes concrete objects that are not present in the image. As illustrated in Figure 1, the model incorrectly mentions a “dining” and a “table” that do not appear in the visual input, revealing a typical failure of visual grounding.

To tackle this challenge, existing studies have explored a range of solutions, including training-based (Yang et al. 2025; Liu et al. 2024a; Shang et al. 2025; Dai et al. 2025; Zhao et al. 2025) and decoding-based (Wu et al. 2025; Yin et al. 2024; Chuang et al. 2024; Tang et al. 2025; Leng



Figure 1: **An illustration of object hallucination in multimodal generation.** The upper response, generated by the LLaVA model (Liu et al. 2024b) using greedy decoding, hallucinates non-existent objects—“dining” and “table” (highlighted in red)—which are absent from the image. This reveals a typical failure of visual grounding. In contrast, the lower response, produced by LISA, provides a faithful and grounded description, free from **object hallucination**.

et al. 2024; Huang et al. 2024; Wang et al. 2025; Cao et al. 2025; Xie et al. 2025; Hu et al. 2025; Li et al. 2025a; Ruan et al. 2025) approaches. Training-based methods typically optimize model parameters using hallucination-sensitive supervision. OPA-DPO (Yang et al. 2025), for instance, distills visual preference signals from the closed-source GPT-4V to guide model responses toward human-aligned outputs, but this reliance on proprietary systems limits reproducibility and transparency. In contrast, LRV-Instruction (Liu et al. 2024a) curates a large-scale instruction dataset comprising both grounded and hallucination-inducing prompts to enhance robustness via instruction tuning. Despite avoiding manual annotation, these approaches require substantial

effort for dataset construction and model adaptation, constraining their scalability.

Given the high cost and limited scalability of training-based methods, decoding-time strategies have emerged as scalable, training-free alternatives for hallucination mitigation. Some methods leverage external tools to enhance reasoning or verification. Bottom-Up Holistic Reasoning (Wu et al. 2025) uses external tools such as scene graph parsers, object detectors, and web search to perform structured reasoning during decoding, while Woodpecker (Yin et al. 2024) performs post-hoc multi-stage analysis to detect and correct hallucinated outputs. Other approaches focus on internal model behavior. DoLa (Chuang et al. 2024) contrasts token confidence across layers to suppress unsupported outputs; TAME (Tang et al. 2025) regularizes the query-key eigenspectrum to stabilize signal propagation; VCD (Leng et al. 2024) applies contrastive constraints on matched and mismatched visual regions; OPERA (Huang et al. 2024) re-decodes with penalties to discourage ungrounded content; and DeCo (Wang et al. 2025) fuses intermediate-layer logits to guide more grounded generation. However, most existing decoding methods treat all transformer layers as equally informative (Huang et al. 2025; Cho et al. 2025; Ru et al. 2024; Fu et al. 2025; Chen et al. 2025), without considering their functional differences. Based on empirical analysis of model behaviors across layers, we observe that MLLMs exhibit internal functional hierarchy: shallow layers contribute to visual grounding, middle layers encode semantic context, and deep layers tend to amplify unstable signals. These observations underscore the need for decoding strategies that explicitly account for layer-wise functional roles and modulate information across layers accordingly.

Building on this observation, we propose **LISA** (*a Layer-wise Integration and Suppression Approach*), a training-free decoding strategy designed to mitigate object hallucination. LISA exploits layer-wise functional roles in multimodal transformers, partitioning the model into shallow, middle, and deep zones for grounding, semantic integration, and spurious-signal suppression. It stabilizes the attention weights via *layer-wise spectral modulation*, suppressing over-amplified, unstable signals in deeper layers while preserving stable alignment cues in shallower ones. Token-level logits from representative layers are then aggregated through cross-layer fusion and token-wise anchor routing, ensuring more reliable and faithful generation.

LISA is fully **plug-and-play**, requiring no retraining or architectural modification, and can be seamlessly applied to a variety of MLLMs. We evaluate LISA on several hallucination benchmarks, including CHAIR (Rohrbach et al. 2018), POPE (Li et al. 2023), AMBER (Wang et al. 2023), and MME (Fu et al. 2023), demonstrating consistent hallucination reduction and improved factual consistency. Our method offers a lightweight yet effective approach to enhance the reliability of multimodal generation.

Our contributions are summarized as follows:

- We identify a key limitation of existing decoding-time approaches: they overlook the layer-wise functional roles of transformer layers, leading to suboptimal integration of layer-wise representations and insufficient modulation

of spectral instability during decoding.

- We propose LISA, a training-free decoding framework that leverages the functional hierarchy of MLLMs. By applying layer-wise spectral modulation to stabilize attention dynamics and fusing logits across selected anchor layers, LISA effectively mitigates hallucinations.
- We conduct comprehensive evaluations on four hallucination benchmarks across multiple MLLMs. LISA consistently reduces hallucinations while preserving generation quality and demonstrates strong compatibility with diverse architectures and decoding strategies.

Related Work

Hallucination in MLLMs

Multimodal Large Language Models (MLLMs) unify visual and linguistic understanding to handle tasks such as image captioning and visual question answering. Despite advances in instruction tuning and cross-modal alignment (Liu et al. 2024b; Dai et al. 2023; Bai et al. 2023; Zhuang et al. 2025a; Zhang et al. 2025a; Yin et al. 2025; Zhuang et al. 2025b; Li et al. 2025b), MLLMs still frequently hallucinate object-level details that are unsupported by the input image, especially in complex or ambiguous scenes. These failures expose fundamental limitations in visual grounding and continue to drive research on hallucination mitigation.

Hallucination Mitigation for MLLMs

Decoding-time strategies have received increasing attention for their training-free and plug-and-play characteristics. Methods such as DoLa (Chuang et al. 2024), DeCo (Wang et al. 2025), OPERA (Huang et al. 2024), and VCD (Leng et al. 2024) intervene during generation by reweighting logits, anchoring shallow-layer signals, or reranking outputs. While effective, these approaches often ignore the functional hierarchy of transformer layers, treating them as uniformly informative.

In contrast, our method LISA introduces a layer-wise perspective on the transformer architecture. Instead of treating all layers equivalently, LISA explicitly partitions the model into shallow, middle, and deep zones based on their observed roles in grounding visual entities, maintaining contextual coherence, and refining linguistic details. To stabilize generation, LISA performs targeted spectral modulation across these zones, dynamically suppressing unstable signals while preserving grounded information. This layer-wise intervention enables more precise control over the generation process and improves alignment between textual outputs and visual evidence.

Layer-wise Structure in MLLMs

Zhang et al. (2025c) conducted attention ablation analyses, revealing a staged organization within MLLMs: shallow layers propagate general visual features, intermediate layers refine object-specific details, and later layers consolidate task-specific semantics. While their investigation offers valuable interpretability, it remains primarily descriptive, abstaining from a systematic exploration of how to leverage this hierarchical structure to enhance generative capabilities.

In contrast, our proposed LISA builds on this insight by explicitly treating the transformer as a functionally hierarchical system—dividing it into shallow, middle, and deep zones—and actively stabilizing cross-layer representations through layer-wise spectral suppression and cross-layer fusion. This design transforms descriptive observations into an effective, plug-and-play decoding mechanism that improves generation robustness without requiring retraining or architectural changes.

Methodology

Why Layer Matters: A Hierarchical Perspective

MLLMs produce textual responses by progressively transforming internal representations through a stack of transformer layers. While prior work (Zhang et al. 2025c) has primarily examined where modality fusion occurs, we shift focus to how grounded and hallucinated contents propagate through different layers during decoding.

Figure 2 illustrates representative layer-wise token probabilities for hallucinated and non-hallucinated examples. Consistent with prior findings (Wang et al. 2025), hallucinated tokens often maintain persistently high probabilities in deeper layers, amplifying spurious signals. Interestingly, valid words that are split into multiple sub-tokens (e.g., *cake* → “c”, “ake”) can also show similar high-probability plateaus, even when they are correctly grounded. This phenomenon suggests that persistent activations in deeper layers do not always imply hallucinations, underscoring the importance of a robust, layer-wise mechanism that can dampen unstable signals without over-suppressing legitimate content.

To interpret this behavior further, we plot a representative query spectral energy curve in Figure 3. We observe that in the shallow layers, the spectral energy remains low and dispersed. This zone primarily serves to preserve the input features, acting as a robust foundation for subsequent processing. As signals propagate through the middle layers, a steady increase in spectral energy indicates the progressive integration of semantic information. This is where the model performs crucial cross-modal fusion, blending visual and textual cues to build a coherent, grounded representation of the input. However, a distinct and problematic pattern emerges in the deeper layers. Here, we frequently observe abrupt spikes in spectral energy that correlate with the model’s confidence in specific tokens. Consistent with prior work on large models such as LLaVA (Liu et al. 2024b), these spikes often align with the model’s overconfident predictions, leading to the generation of spurious or hallucinatory content. While some of these spikes may correspond to legitimate phenomena like token splits for valid words, they more typically signal the amplification of unstable representations. This observation underscores a critical challenge: distinguishing between beneficial amplification of grounded signals and detrimental amplification of spurious ones. This is why LISA adopts a layer-wise spectral modulation strategy. Rather than rigidly distinguishing each case, it adaptively controls layer-wise signals to mitigate these deep-layer activations while preserving valid structures from more stable shallow and middle layers.

Figure 4 demonstrates the practical impact of our spectral modulation. Compared with existing MLLMs (Liu et al. 2024b; Dai et al. 2023; Bai et al. 2023, 2025), LISA effectively suppresses final-layer overactivation for hallucinated tokens and promotes a more balanced layer-wise activation pattern, resulting in more reliable and faithful outputs.

Together, these observations suggest a functional hierarchy: shallow layers preserve inputs; middle layers integrate grounded semantics; deep layers tend to amplify spurious signals. Motivated by this hierarchical view, we propose LISA, which explicitly partitions the transformer into three spectral zones—preservation, interaction, and suppression, as shown in Figure 5. By combining layer-wise spectral modulation, cross-layer fusion, and token-wise anchor routing, LISA adaptively balances final-layer representation capacity with stability, mitigating hallucinations without re-training or changing parameters of MLLMs.

Spectral Modulation for Layer-wise Stability

Motivated by prior insights (Tang et al. 2025) that controlling the query-key eigenspectrum can stabilize generation, we introduce LISA’s first core mechanism: *Spectral Modulation (SM)*. It combines layer-wise spectral suppression and cross-layer token fusion to mitigate hallucinations in multi-modal generation. This approach builds on the observation that transformer layers exhibit layer-wise functional roles, and that different layers contribute differently to the final output.

Layer-wise Spectral Suppression. For each transformer layer l , we define its spectral energy as the squared Frobenius norm of its query and key matrices:

$$\begin{aligned} \text{Tr}_Q^{(l)} &= \|\mathbf{Q}^{(l)}\|_F^2 = \text{Tr}(\mathbf{Q}^{(l)} \mathbf{Q}^{(l)\top}), \\ \text{Tr}_K^{(l)} &= \|\mathbf{K}^{(l)}\|_F^2 = \text{Tr}(\mathbf{K}^{(l)} \mathbf{K}^{(l)\top}). \end{aligned} \quad (1)$$

As shown in Figure 3, spectral energy remains low and dispersed in shallow layers (preservation zone), gradually increases in middle layers (interaction zone) as semantic fusion occurs, and often shows abrupt spikes in deep layers (suppression zone), which we have found to align with the emergence of hallucinations.

To suppress unstable activations and prevent them from dominating the generation process, we apply a dynamic spectral modulation factor to the scaled dot-product attention. This mechanism is designed to constrain high-energy spikes while minimally affecting stable, low-energy activations:

$$\begin{aligned} \lambda_Q^{(l)} &= 1 + \frac{\gamma^{(l)}}{\log(\text{Tr}_Q^{(l)} + \epsilon)}, \\ \lambda_K^{(l)} &= 1 + \frac{\gamma^{(l)}}{\log(\text{Tr}_K^{(l)} + \epsilon)}, \end{aligned} \quad (2)$$

where ϵ is a small positive constant to ensure numerical stability. The suppression strength parameter, γ , is not a fixed value but is dynamically set based on the layer index l . We model this relationship using a simple monotonically increasing function that reflects the functional hierarchy of the transformer.

$$\gamma^{(l)} = \gamma_{\min} + (\gamma_{\max} - \gamma_{\min}) \cdot \frac{l}{L}, \quad (3)$$

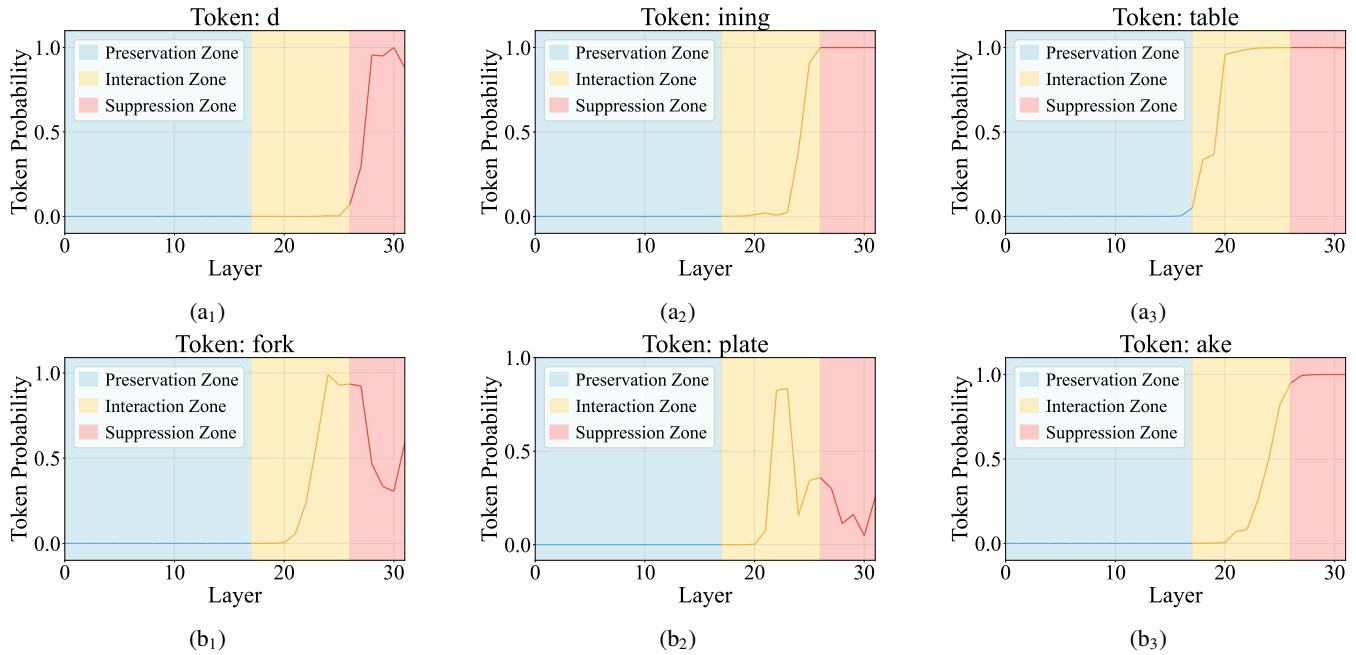


Figure 2: **Layer-wise token probabilities.** The token probability is calculated by applying the Softmax function to the raw logits of the token at each layer. Subfigures (a₁)–(a₃) show hallucinated tokens; subfigures (b₁)–(b₃) show non-hallucinated tokens. Y-axis: token probability; X-axis: layer index (0–31).

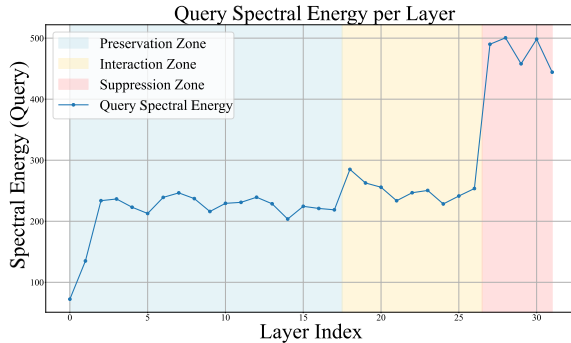


Figure 3: **Layer-wise spectral energy during token prediction.** A representative example from a Multimodal Large Language Model (MLLM) shows that query spectral energy varies across layers for a single token generation step, forming three zones: *Preservation* (blue) retains input signals; *Interaction* (yellow) builds semantic fusion; *Suppression* (red) shows spikes linked to hallucination. This pattern motivates layer-wise decoding strategies.

where L is the total number of layers in the model. For the model used in our experiments, L is the total number of decoder layers, which is 32. This linear model is the simplest and most interpretable way to capture the observed monotonic increase in representation change across layers. It requires tuning only two boundary parameters, γ_{\min} and γ_{\max} . Specifically, setting $\gamma_{\min} = 0.0$ ensures the shallowest layers apply no spectral suppression at all, preserving input fi-

delity. $\gamma_{\max} = 0.9$ is empirically chosen as the maximum strength that significantly curtails hallucination while maintaining coherent generation quality. This dynamic approach ensures that the suppression strength increases progressively with layer depth, ranging from a minimum value γ_{\min} for the shallowest layers to a maximum value γ_{\max} for the deepest layers. The modulated attention then becomes:

$$\mathbf{A}^{(l)} = \text{Softmax} \left(\frac{(\lambda_Q^{(l)} \mathbf{Q}^{(l)}) (\lambda_K^{(l)} \mathbf{K}^{(l)})^\top}{\sqrt{d_k}} \right), \quad (4)$$

where d_k is the dimensionality of the query/key vectors. By specifically constraining high-energy spikes in deeper layers, this targeted suppression method mitigates overactivation while preserving the robust representation capacity of the network’s more stable layers.

Cross-layer Token Fusion. Beyond local suppression, LISA globally aggregates stable information through its second core mechanism, *Cross-layer Fusion (CF)*. Rather than relying solely on the final layer or averaging across all layers, CF strategically fuses token states from a carefully selected anchor layer set \mathcal{A} , which consists of representative layers sampled from the three zones. To guide this fusion, we introduce *spectral stability* to measure the reliability of layer representations. It is defined as the inverse of the spectral energy:

$$s^{(l)} = \frac{1}{\text{Tr}_Q^{(l)} + \text{Tr}_K^{(l)} + \epsilon}, \quad (5)$$

where $\text{Tr}_Q^{(l)}$ and $\text{Tr}_K^{(l)}$ denote the spectral trace energies of the query and key matrices, respectively. This metric cap-

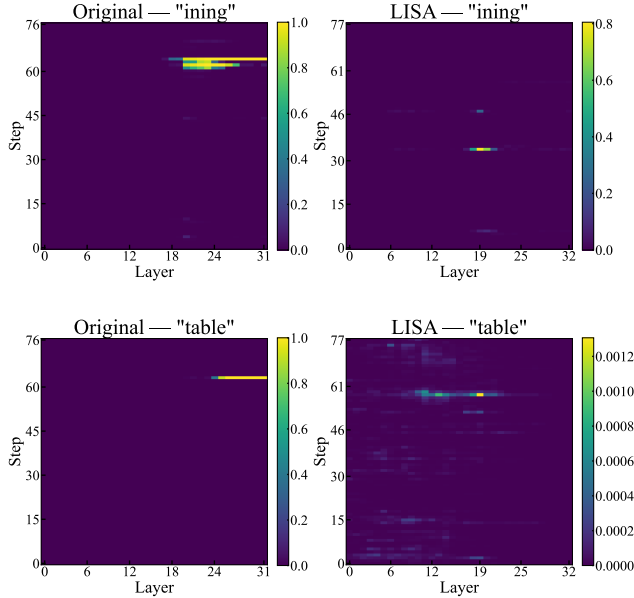


Figure 4: Layer-wise heatmaps of hallucinated tokens. *Left:* Greedy decoding shows sharp final-layer spikes (e.g., “ining”, “table”). *Right:* LISA suppresses unstable activations and distributes confidence across layers.

tures the layer-wise reliability: low energy indicates stable, grounded representations, while high energy indicates volatile, potentially hallucinated representations. Our fusion mechanism leverages this by amplifying stable signals from shallow/middle layers and dampening spurious deep-layer activations. We acknowledge that this strategy may weakly regularize some high-confidence legitimate sub-tokens, but empirically, the resulting net reduction in hallucination significantly outweighs this minimal trade-off.

The fusion weights are normalized to ensure a consistent contribution:

$$\alpha^{(l)} = \frac{s^{(l)}}{\sum_{j \in \mathcal{A}} s^{(j)}}, \quad \sum_{l \in \mathcal{A}} \alpha^{(l)} = 1. \quad (6)$$

The final fused representation, \mathbf{H}_{LISA} , is formulated as a weighted sum of the representations from the anchor layers:

$$\mathbf{H}_{\text{LISA}} = \sum_{l \in \mathcal{A}} \alpha^{(l)} \mathbf{H}^{(l)}. \quad (7)$$

This strategic aggregation amplifies grounded signals from stable layers while dampening unstable ones, leading to more reliable generation outputs.

Layer-wise Token Integration for Stable Generation

Building on stable multi-layer signals, LISA extends this layer-wise design into the decoding stage through its third core mechanism, which we term *Token-wise Soft Fusion (TSF)*. Unlike conventional pipelines that rely solely on

final-layer logits, TSF aligns the generation of each token with the layer-wise spectral pattern: grounded content stabilizes in shallow and intermediate layers, while hallucinations often correlate with unstable deep-layer spikes.

Token-wise Anchor Selection. To leverage this, we first partition the transformer into three zones—preservation, interaction, and suppression—and select representative layers from each zone to form an initial anchor set $\mathcal{A}_{\text{anchor}}$. Crucially, we retrieve the hidden states from these intermediate layers and pass them to the model’s shared final classification head (LM Head) to obtain layer-wise logits ($\mathbf{L}_{\mathbf{H},t}$) and token probabilities. The cross-layer fused representation \mathbf{H}_{LISA} is computed from this set (as defined in Eq. 7), and is then included as an additional candidate for the final token-wise fusion.

The complete set of candidate anchors for logit fusion is therefore:

$$\mathcal{C} = \{\mathbf{H}^{(l)} \mid l \in \mathcal{A}_{\text{anchor}}\} \cup \{\mathbf{H}_{\text{LISA}}\}. \quad (8)$$

Since \mathbf{H}_{LISA} is a fused representation and does not correspond to a single layer index, we define its effective stability, $s(\mathbf{H}_{\text{LISA}})$, as the average spectral stability of its constituent anchor layers:

$$s(\mathbf{H}_{\text{LISA}}) = \frac{1}{|\mathcal{A}_{\text{anchor}}|} \sum_{l \in \mathcal{A}_{\text{anchor}}} s^{(l)}. \quad (9)$$

For each token c considered for generation, the optimal anchor representation \mathbf{H}_c^* is dynamically selected by maximizing spectral stability-weighted probability:

$$\mathbf{H}_c^* = \arg \max_{\mathbf{H} \in \mathcal{C}} (s(\mathbf{H}) \cdot \text{Softmax}(\mathbf{L}_{\mathbf{H},t})_c), \quad (10)$$

where $\mathbf{L}_{\mathbf{H},t}$ is the logit vector obtained by passing \mathbf{H} through the LM Head. The term \mathbf{H}_c^* is the optimal anchor selected specifically for token c , and $s(\mathbf{H})$ is the spectral stability of the source of \mathbf{H} (either $s^{(l)}$ for a single layer or $s(\mathbf{H}_{\text{LISA}})$ for the fused representation). This process ensures that the chosen anchor \mathbf{H}_c^* is the representation that is most stable and provides the highest confidence for the intended token c , aligning the calculation with the mechanism’s core goal.

Soft Logit Fusion. Finally, token logits are fused to balance representation capacity and stability. Since the optimal anchor is token-dependent, the fusion is performed for every candidate token c :

$$\hat{\mathbf{L}}_t(c) = \mathbf{L}_{L,t}(c) + \beta \mathbf{L}_{\mathbf{H}_c^*,t}(c), \quad \beta \in [0, 1]. \quad (11)$$

Here, $\hat{\mathbf{L}}_t(c)$ is the resulting fused logit for token c . The terms $\mathbf{L}_{L,t}(c)$ and $\mathbf{L}_{\mathbf{H}_c^*,t}(c)$ are the logits for token c from the final layer (L) and its selected token-specific anchor (\mathbf{H}_c^*), respectively. β controls the trade-off between the capacity of the final layer and the stability of the selected anchor. This design allows each token to adaptively draw from its own most stable, high-confidence source, thereby mitigating hallucinations across decoding strategies while preserving layer-wise information.

LISA integrates multi-layer signals, enhancing the stability of token generation. By dynamically selecting the most

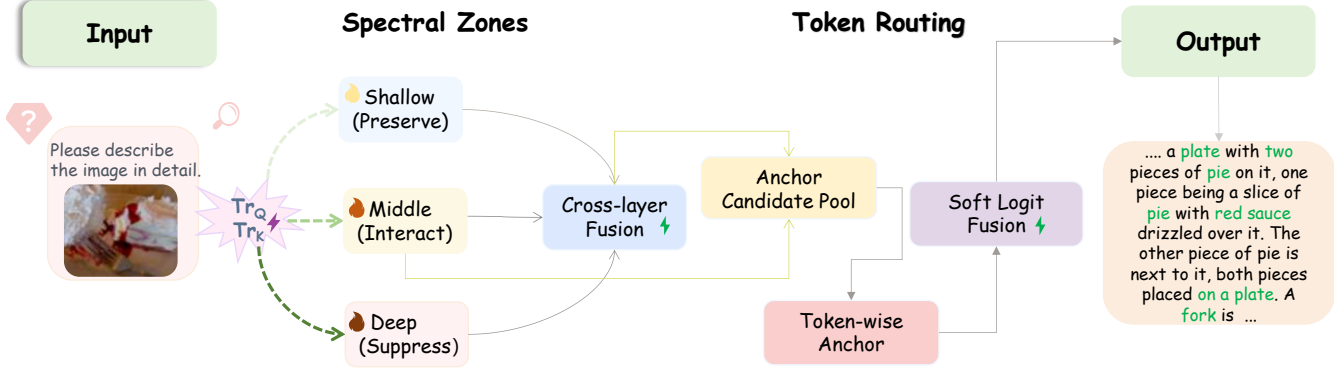


Figure 5: **Overview of LISA.** LISA stabilizes multimodal generation by modulating the layer-wise spectral energy of transformer attention. It partitions layers into three spectral zones—preservation, interaction, and suppression—reflecting the layer-wise spectral energy progression of queries and keys. Layer-wise spectral suppression dynamically scales attention to dampen unstable deep-layer spikes while preserving shallow and middle-layer semantics. Cross-layer token fusion aggregates stable representations across selected anchor layers, weighted by spectral stability. Finally, token-wise anchor selection and soft logit fusion adaptively integrate multi-layer signals during decoding, ensuring each token draws from the most stable layers. Together, LISA combines spectral modulation, anchor-based fusion, and token-wise routing to mitigate hallucinations while retaining layer-wise information.

stable anchor layer based on both spectral stability and token probability, and soft-fusing the logits, LISA minimizes hallucinations and ensures the generation of meaningful, coherent content. Together, these mechanisms yield a robust decoding approach that enhances both accuracy and stability, while preserving layer-wise information throughout the generation process.

Experiments

Experimental Settings

Datasets. We use MSCOCO (Lin et al. 2014), which contains diverse everyday scenes with human-annotated captions. Only images are used for inference; captions are for evaluation.

Baselines. We compare LISA with standard decoding strategies (e.g., greedy decoding, beam search, and nucleus sampling) and recent decoding-time hallucination mitigation methods, including DoLa (Chuang et al. 2024), DeCo (Wang et al. 2025), VCD (Leng et al. 2024), and OPERA (Huang et al. 2024).

Backbone Models. We evaluate our method with four MLLMs: LLaVA (Liu et al. 2024b), InstructBLIP (Dai et al. 2023), Qwen-VL (Bai et al. 2023), and Qwen2.5-VL (Bai et al. 2025), all used in frozen form without fine-tuning.

Implementation Details. For a 32-layer decoder-only language model, the dynamic spectral suppression parameter $\gamma^{(l)}$ is governed by $\gamma_{\min} = 0.0$ and $\gamma_{\max} = 0.9$ (validated in Figure 7).

To ensure reproducibility, we formally define the three functional zones (defined by spectral energy) using a proportional split based on the total layer count L :

- **Preservation Zone:** $0 \leq l \leq \lfloor 0.30 \cdot L \rfloor$;
- **Interaction Zone:** $\lfloor 0.30 \cdot L \rfloor < l \leq \lfloor 0.85 \cdot L \rfloor$;

Hyperparameter	Value	Description
Beam size	5	Beam size
Temperature	0.7	Sampling temperature
Max tokens	512	Maximum generation length
β	0.6	Token-wise fusion weight
ϵ	10^{-7}	Spectral stabilizer
γ_{\min}	0.0	Minimum suppression strength for γ
γ_{\max}	0.9	Maximum suppression strength for γ

Table 1: Main hyperparameters used in LISA. The value of γ is dynamically set based on the function defined in Eq. 3.

- **Suppression Zone:** $\lfloor 0.85 \cdot L \rfloor < l \leq L$.

This layer-wise hierarchical division is consistent with findings that deeper layers are more susceptible to generating non-factual content (Wang et al. 2025). Main decoding hyperparameters are given in Table 1.

Evaluation Benchmarks

CHAIR. The Caption Hallucination Assessment with Image Relevance (CHAIR) (Rohrbach et al. 2018) evaluates object hallucination in captions by comparing generated object mentions with ground-truth labels. It is defined as:

$$\text{CHAIR}_I = \frac{|\text{Hallucinated Objects}|}{|\text{Mentioned Objects}|},$$

$$\text{CHAIR}_S = \frac{|\text{Captions with Hallucinations}|}{|\text{All Captions}|}.$$

Following Huang et al. (2024), we evaluate on 500 MSCOCO 2014 validation images, averaging the results over 3 runs with different random seeds, using the caption prompt: “Please describe the image in detail.”

Decoding	Method	LLaVA-1.5		InstructBLIP		Qwen-VL	
		CHAIR _S ↓	CHAIR _I ↓	CHAIR _S ↓	CHAIR _I ↓	CHAIR _S ↓	CHAIR _I ↓
Greedy	Vanilla	45.0	14.7	58.8	23.7	46.0	12.5
	DoLa	47.8	13.8	48.4	15.9	46.8	12.9
	DeCo	37.8	11.1	41.2	14.4	42.2	10.7
	LISA	34.2 ↓10.8	10.4 ↓4.3	31.6 ↓27.2	10.9 ↓12.8	29.0 ↓17.0	9.2 ↓3.3
Beam	Vanilla	48.8	13.9	55.6	15.8	41.8	10.8
	OPERA	44.6	12.8	46.4	14.2	34.6	9.5
	DeCo	33.0	9.7	43.8	12.7	32.0	8.7
	LISA	29.2 ↓19.6	9.1 ↓4.8	31.0 ↓24.6	11.6 ↓1.1	20.4 ↓21.4	7.4 ↓3.4
Nucleus	Vanilla	48.8	14.2	54.6	24.8	49.2	13.1
	VCD	54.0	16.0	58.0	17.0	46.4	11.9
	DeCo	42.8	13.2	43.6	12.9 ↓11.9	43.8	11.8
	LISA	39.0 ↓9.8	11.6 ↓2.6	39.4 ↓15.2	16.3	30.2 ↓19.0	10.3 ↓2.8

Table 2: **CHAIR hallucination evaluation results** for **LLaVA-1.5**, **InstructBLIP**, and **Qwen-VL** across different decoding strategies. Lower scores on CHAIR_S and CHAIR_I indicate fewer hallucinations. OPERA is a beam-search-based method; VCD is designed for nucleus sampling; DeCo is a general decoding-compatible approach. LISA denotes our method, and is applied consistently across all settings.

Decoding	Method	CHAIR↓	Cover↑	Hal.↓	Cog.↓
Greedy	Vanilla	8.2	48.9	34.3	4.0
	DoLa	8.0	50.8	37.5	4.3
	DeCo	6.6	47.5	28.1	2.8
	LISA	6.5 ↓1.7	47.2 ↓1.7	23.1 ↓11.2	1.9 ↓2.1
Beam	Vanilla	7.1	50.7	32.4	3.8
	OPERA	6.4	49.0	27.5	2.9
	DeCo	6.3	46.8	25.1	2.4
	LISA	5.9 ↓1.2	45.6 ↓5.1	21.9 ↓10.5	2.0 ↓1.8
Nucleus	Vanilla	10.2	50.2	43.3	4.5
	VCD	9.0	51.7	40.2	4.4
	DeCo	8.3	48.0	37.5	3.4
	LISA	7.2 ↓3.0	47.6 ↓2.6	28.8 ↓14.5	2.6 ↓1.9

Table 3: AMBER evaluation results of **LLaVA-1.5** under different decoding strategies. LISA consistently reduces hallucination-related metrics—CHAIR (hallucinated object rate), Hal. (rate of hallucinated responses), and Cog. (alignment with human cognitive biases)—while incurring a slight decrease in Cover, which quantifies the proportion of ground-truth objects correctly mentioned in the response.

AMBER. AMBER (Wang et al. 2023) evaluates hallucinations in image captions by assessing hallucinated object rate (CHAIR), coverage of ground-truth objects (Cover), proportion of hallucinated responses (Hal.), and tendency to mention cognitively biased objects (Cog.). Lower scores for CHAIR, Hal., and Cog. indicate fewer hallucinations, while a higher Cover score reflects stronger grounding.

MME. The MME benchmark (Fu et al. 2023) evaluates the general capabilities of multimodal large language models across 14 subskills, including OCR, object recognition, spatial relations, and commonsense reasoning. It uses multiple-choice questions on natural images. We follow the official protocol and report overall accuracy.

POPE. The Polling-based Object Probing Evaluation (POPE) (Li et al. 2023) assesses hallucination through a binary question-answering format. For each image, the model answers whether a queried object exists in the scene. Performance is measured using the standard F1 score.

To evaluate robustness, POPE splits queried objects into

three subsets: random (arbitrary samples), popular (frequent objects), and adversarial (visually similar to ground-truth). Each subset includes 500 MSCOCO images with six binary questions per image.

Performance Analysis

We evaluate LISA using the four benchmarks introduced above—CHAIR, AMBER, POPE, and MME—which together capture diverse facets of generation reliability, including hallucination mitigation, visual grounding, and factual consistency across different decoding strategies and model families.

Robust Hallucination Mitigation. Table 2 shows that LISA consistently reduces hallucinated object mentions (CHAIR_S, CHAIR_I) across different models and decoding strategies on the CHAIR benchmark. These improvements are particularly evident under beam search, where LISA surpasses existing decoding-time approaches such as DoLa and DeCo, highlighting its effectiveness under conditions most prone to hallucination errors.

Similarly, as shown in Table 3, LISA significantly reduces hallucination metrics (Hal. and Cog.) while preserving grounded object coverage (Cover), demonstrating robustness even in tasks requiring commonsense and spatial reasoning.

Improved Visual Grounding and Recall. As shown in Table 4, LISA consistently improves F1 scores on the POPE benchmark across all evaluated MLLMs, demonstrating enhanced grounding to actual object presence. While initially developed to stabilize caption generation via layer-wise spectral control, LISA also enhances binary yes/no existence prediction, demonstrating its generalizability across output formats. Additional results on Qwen2.5-VL confirm that the layer-wise design of LISA reliably improves object recall and grounding under various decoding strategies.

Consistent Improvements across Tasks. Finally, as shown in Figure 6, LISA achieves the highest overall score

Method	LLaVA-1.5	InstructBLIP	Qwen-VL
Greedy	82.2	80.0	85.2
Nucleus	83.1	79.8	84.5
Beam	84.9	84.4	85.3
DeCo	85.4	81.8	85.2
DoLa	83.2	83.4	85.8
VCD	83.1	79.9	84.7
OPERA	85.4	84.8	86.1
LISA	86.7 $\uparrow 4.5$	84.9 $\uparrow 5.1$	86.7 $\uparrow 2.2$

Table 4: POPE F1 scores of **LLaVA-1.5**, **InstructBLIP**, and **Qwen-VL** under various decoding strategies. Higher scores indicate stronger alignment with object existence. For fair comparison, LISA results are obtained under nucleus sampling.

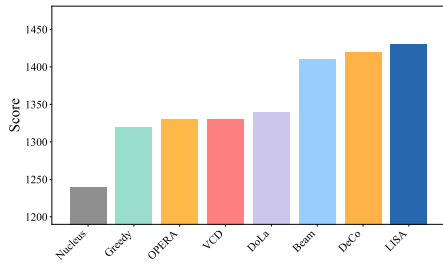


Figure 6: **MME benchmark results.** LISA outperforms standard decoding (i.e., greedy, beam, nucleus) and recent mitigation methods (i.e., DoLa, VCD, OPERA, DeCo).

on the MME benchmark among recent decoding-time hallucination mitigation techniques, demonstrating robust performance for tasks that demand broader multimodal understanding, including spatial reasoning, attribute alignment, and fine-grained object grounding.

Across benchmarks and decoding strategies, LISA consistently enhances visual grounding and generation stability across models, offering a practical, training-free solution for mitigating hallucinations in real-world MLLM applications.

Hyperparameter Study

To optimize the LISA framework, we study two critical parameters: the maximum suppression strength (γ_{\max}) for Spectral Modulation (SM) and the soft logit fusion weight (β) for Token-wise Soft Fusion (TSF). All experiments here used LLaVA-1.5.

Effect of Maximum Suppression Strength (γ_{\max}). As shown in Figure 7, the CHAIR_S score across all decoding strategies performs best when γ_{\max} is in the upper-middle range. The curve shows a broad region of strong performance, indicating that the spectral modulation mechanism is robust to parameter choices. High γ_{\max} values eventually lead to performance saturation and decline, which confirms that over-suppression harms coherence by removing necessary spectral components. We select γ_{\max} at the optimal trade-off point to maximize hallucination mitigation while preserving essential information.

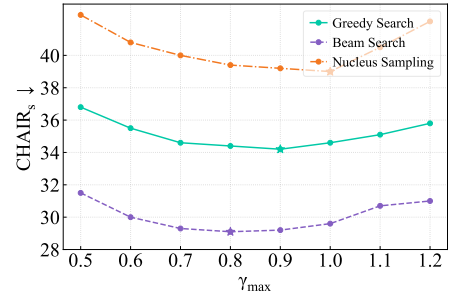


Figure 7: Hyperparameter study on the maximum suppression strength (γ_{\max}). The CHAIR_S score (lower is better) is shown as a function of γ_{\max} , validating $\gamma_{\max} = 0.9$ as the optimal trade-off point.

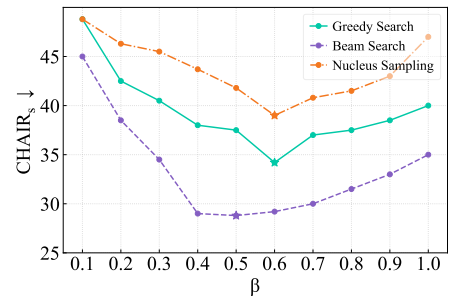


Figure 8: Hyperparameter study on the soft logit fusion weight (β).

Effect of Logit Fusion Weight (β). The weight β controls the trade-off between the raw information from the final layer and the stabilized prediction derived from the cross-layer anchor. As illustrated in Figure 8, performance exhibits a clear concave trend, which validates the necessity of a fusion mechanism:

1. Optimal performance is consistently achieved when β is set to the middle range, which confirms that a balanced contribution from both the final layer and the stable anchor is critical for maximum correction.
2. Performance begins to decline when β deviates significantly from the optimal range. This demonstrates that either insufficient stability at low β or over-reliance on the anchor at high β reduces the overall prediction quality.

Based on this consistent peak, we set the soft logit fusion weight to $\beta = 0.6$.

Ablation Study

To rigorously evaluate the contribution of each core mechanism within the LISA framework, we perform an ablation study using Qwen2.5-VL as our testbed. LISA comprises three main innovations: Spectral Modulation (SM), Cross-layer Fusion (CF), and Token-wise Soft Fusion (TSF). The results, summarized in Table 5, validate that the combination of these layer-wise controls is essential for maximizing hallucination reduction and ensuring robustness across various decoding settings.

Variant	SM	CF	TSF	Greedy	Beam	Nucleus
LISA	✓	✓	✓	85.04	87.09	85.36
LISA w/o SM	✗	✓	✓	84.11	83.81	84.24
LISA w/o CF	✓	✗	✓	84.67	85.54	84.83
LISA w/o TSF	✓	✓	✗	84.87	86.52	85.19
Vanilla	✗	✗	✗	83.93	84.20	84.10

Table 5: Ablation study of LISA’s core components on **Qwen2.5-VL**. The table reports the average POPE F1 score (↑) across three decoding strategies (Greedy, Beam, Nucleus), validating that the layered combination of **SM** (Spectral Modulation), **CF** (Cross-layer Fusion), and **TSF** (Token-wise Soft Fusion) is essential for maximizing hallucination mitigation and grounding.

Experimental Variants. We compare the full LISA framework with the following essential variants:

1. **LISA (full):** The complete framework, including Spectral Modulation (SM), Cross-layer Fusion (CF), and Token-wise Soft Fusion (TSF).
2. **LISA w/o SM (disabling stabilization):** We disable the *Spectral Modulation (SM)* mechanism by setting $\gamma_{\max} = 0.0$. This variant performs fusion and selection based purely on the raw spectral energy of the unstable representations.
3. **LISA w/o CF (disabling aggregation):** This variant disables *Cross-layer Fusion (CF)*. Specifically, we prevent the creation and use of the stable fused representation \mathbf{H}_{LISA} , forcing the subsequent TSF module to select only from individual layer representations.
4. **LISA w/o TSF (disabling adaptive routing):** We perform SM and compute the stable representation \mathbf{H}_{LISA} , but bypass the final *Token-wise Soft Fusion (TSF)* step. Instead, the model relies only on the final layer logits ($H^{(L)}$).

Results and Analysis. As shown in Table 5, the complete LISA framework consistently achieves the best average POPE F1 score across all tested decoding strategies, confirming the effectiveness of integrating its three controls. The ablation results validate the necessity and layer-wise function of each component:

1. Removing *Spectral Modulation (SM)* causes the most severe performance degradation, sometimes falling below the vanilla baseline. This highlights SM as the indispensable first step for stabilizing the model.
2. Excluding *Cross-layer Fusion (CF)* results in a notable decline. CF is necessary for robust multi-layer integration, as it aggregates stabilized layers into a reliable anchor (\mathbf{H}_{LISA}).
3. Removing *Token-wise Soft Fusion (TSF)* causes a modest yet consistent drop. TSF acts as the final adaptive routing mechanism, ensuring the stable representation is utilized effectively, especially under high-risk decoding strategies.

In summary, the results confirm that LISA functions as a layered system: SM prevents destabilization, CF enhances robustness through multi-layer aggregation, and TSF adaptively exploits this stability during decoding. Together, these

components yield consistent improvements over the vanilla baseline.

Conclusion

We present LISA, a training-free decoding approach that mitigates hallucinations in MLLMs through **layer-wise integration and suppression**. Our deep analysis of token trajectories and spectral energy patterns uncovers functional distinctions across layers, motivating a layer-wise decoding design that preserves stable signals, facilitates semantic fusion, and suppresses unstable activations.

LISA introduces no additional training cost and is broadly applicable to existing MLLMs. Extensive experiments across multiple benchmarks validate its effectiveness in reducing hallucinations and enhancing output fidelity. These findings highlight the potential of layer-aware decoding and open new avenues for dynamic layer selection, adaptive routing, and post-hoc consistency verification.

References

Bai, J.; Bai, S.; Yang, S.; Wang, S.; Tan, S.; Wang, P.; Lin, J.; Zhou, C.; and Zhou, J. 2023. Qwen-VL: A Frontier Large Vision-Language Model with Versatile Abilities. *arXiv preprint arXiv:2308.12966*.

Bai, S.; Chen, K.; Liu, X.; Wang, J.; Ge, W.; Song, S.; Dang, K.; Wang, P.; Wang, S.; Tang, J.; Zhong, H.; Zhu, Y.; Yang, M.; Li, Z.; Wan, J.; Wang, P.; Ding, W.; Fu, Z.; Xu, Y.; Ye, J.; Zhang, X.; Xie, T.; Cheng, Z.; Zhang, H.; Yang, Z.; Xu, H.; and Lin, J. 2025. Qwen2.5-VL Technical Report. *arXiv preprint arXiv:2502.13923*.

Cao, Z.; He, Y.; Liu, A.; Xie, J.; Wang, Z.; and Chen, F. 2025. CoFi-Dec: Hallucination-Resistant Decoding via Coarse-to-Fine Generative Feedback in Large Vision-Language Models. In *Proceedings of the 33rd ACM International Conference on Multimedia, MM 2025*, 10709–10718.

Chen, J.; Zhang, T.; Huang, S.; Niu, Y.; Zhang, L.; Wen, L.; and Hu, X. 2025. ICT: Image-Object Cross-Level Trusted Intervention for Mitigating Object Hallucination in Large Vision-Language Models. In *IEEE/CVF Conference on Computer Vision and Pattern Recognition, CVPR 2025*, 4209–4221.

Cho, Y.; Kim, K.; Hwang, T.; and Cho, S. 2025. Do You Keep an Eye on What I Ask? Mitigating Multimodal Hallucination via Attention-Guided Ensemble Decoding. In *The Thirteenth International Conference on Learning Representations, ICLR 2025*.

Chuang, Y.; Xie, Y.; Luo, H.; Kim, Y.; Glass, J. R.; and He, P. 2024. DoLa: Decoding by Contrasting Layers Improves Factuality in Large Language Models. In *The Twelfth International Conference on Learning Representations, ICLR 2024*.

Dai, W.; Li, J.; Li, D.; Tiong, A. M. H.; Zhao, J.; Wang, W.; Li, B.; Fung, P.; and Hoi, S. C. H. 2023. InstructBLIP: Towards General-purpose Vision-Language Models with Instruction Tuning. In *Advances in Neural Information Processing Systems 36: Annual Conference on Neural Information Processing Systems 2023, NeurIPS 2023*.

Dai, Z.; Li, X.; Zhang, S.; Wu, Y.; and Li, J. 2025. See Different, Think Better: Visual Variations Mitigating Hallucinations in LVLMs. In *Proceedings of the 33rd ACM International Conference on Multimedia, MM 2025*, 3310–3319.

Floridi, L.; and Chiriatti, M. 2020. GPT-3: Its Nature, Scope, Limits, and Consequences. *Minds Mach.*, 30(4): 681–694.

Fu, C.; Chen, P.; Shen, Y.; Qin, Y.; Zhang, M.; Lin, X.; Yang, J.; Zheng, X.; Li, K.; Sun, X.; Wu, Y.; and Ji, R. 2023. MME: A Comprehensive Evaluation Benchmark for Multimodal Large Language Models. *arXiv preprint arXiv:2306.13394*.

Fu, J.; Huangfu, S.; Fei, H.; Shen, X.; Hooi, B.; Qiu, X.; and Ng, S. 2025. CHiP: Cross-modal Hierarchical Direct Preference Optimization for Multimodal LLMs. In *The Thirteenth International Conference on Learning Representations, ICLR 2025*.

Hu, N.; Duan, X.; Zhang, J.; and Kang, G. 2025. Enhancing Visual Reliance in Text Generation: A Bayesian Perspective on Mitigating Hallucination in Large Vision-Language Models. In *Proceedings of the 33rd ACM International Conference on Multimedia, MM 2025*, 4778–4787.

Huang, Q.; Dong, X.; Zhang, P.; Wang, B.; He, C.; Wang, J.; Lin, D.; Zhang, W.; and Yu, N. 2024. OPERA: Alleviating Hallucination in Multi-Modal Large Language Models via Over-Trust Penalty and Retrospection-Allocation. In *IEEE/CVF Conference on Computer Vision and Pattern Recognition, CVPR 2024*, 13418–13427.

Huang, W.; Zhai, Z.; Shen, Y.; Cao, S.; Zhao, F.; Xu, X.; Ye, Z.; and Lin, S. 2025. Dynamic-LLaVA: Efficient Multimodal Large Language Models via Dynamic Vision-language Context Sparsification. In *The Thirteenth International Conference on Learning Representations, ICLR 2025*.

Leng, S.; Zhang, H.; Chen, G.; Li, X.; Lu, S.; Miao, C.; and Bing, L. 2024. Mitigating Object Hallucinations in Large Vision-Language Models through Visual Contrastive Decoding. In *IEEE/CVF Conference on Computer Vision and Pattern Recognition, CVPR 2024*, 13872–13882.

Li, J.; Wu, M.; Jin, Z.; Chen, H.; Ji, J.; Sun, X.; Cao, L.; and Ji, R. 2025a. MIHBench: Benchmarking and Mitigating Multi-Image Hallucinations in Multimodal Large Language Models. In *Proceedings of the 33rd ACM International Conference on Multimedia, MM 2025*, 3143–3152.

Li, S.; Xu, X.; Meng, W.; Song, J.; Peng, C.; and Shen, H. T. 2025b. Mitigating Hallucinations in Large Vision-Language Models via Reasoning Uncertainty-Guided Refinement. *IEEE Trans. Multim.*, 27: 7380–7391.

Li, Y.; Du, Y.; Zhou, K.; Wang, J.; Zhao, W. X.; and Wen, J. 2023. Evaluating Object Hallucination in Large Vision-Language Models. In *Proceedings of the 2023 Conference on Empirical Methods in Natural Language Processing, EMNLP 2023*, 292–305.

Lin, T.; Maire, M.; Belongie, S. J.; Hays, J.; Perona, P.; Ramanan, D.; Dollár, P.; and Zitnick, C. L. 2014. Microsoft COCO: Common Objects in Context. In *Computer Vision - ECCV 2014 - 13th European Conference, Zurich, Switzerland, September 6-12, 2014, Proceedings, Part V*, 740–755.

Liu, F.; Lin, K.; Li, L.; Wang, J.; Yacoob, Y.; and Wang, L. 2024a. Mitigating Hallucination in Large Multi-Modal Models via Robust Instruction Tuning. In *The Twelfth International Conference on Learning Representations, ICLR 2024*.

Liu, H.; Li, C.; Li, Y.; and Lee, Y. J. 2024b. Improved Baselines with Visual Instruction Tuning. In *IEEE/CVF Conference on Computer Vision and Pattern Recognition, CVPR 2024*, 26286–26296.

OpenAI. 2023. GPT-4 Technical Report. *arXiv preprint arXiv:2303.08774*.

Rohrbach, A.; Hendricks, L. A.; Burns, K.; Darrell, T.; and Saenko, K. 2018. Object Hallucination in Image Captioning. In *Proceedings of the 2018 Conference on Empirical Methods in Natural Language Processing*, 4035–4045.

Ru, J.; Tian, J.; Xiao, C.; Li, J.; and Shen, H. T. 2024. Imbalanced Open Set Domain Adaptation via Moving-Threshold Estimation and Gradual Alignment. *IEEE Trans. Multim.*, 26: 2504–2514.

Ru, J.; Xie, Y.; Zhuang, X.; Yin, Y.; and Zou, Y. 2025. Do we really have to filter out random noise in pre-training data for language models? *arXiv preprint arXiv:2502.06604*.

Ruan, J.; Zhang, Z.; Gao, J.; Yuan, W.; Liu, T.; and Fu, Y. 2025. MPI-CD: Multi-Path Information Contrastive Decoding for Mitigating Hallucinations in Large Vision-Language Models. In *Proceedings of the 33rd ACM International Conference on Multimedia, MM 2025*, 4251–4260.

Shang, Y.; Zeng, X.; Zhu, Y.; Yang, X.; Fang, Z.; Zhang, J.; Chen, J.; Liu, Z.; and Tian, Y. 2025. From Pixels to Tokens: Revisiting Object Hallucinations in Large Vision-Language Models. In *Proceedings of the 33rd ACM International Conference on Multimedia, MM 2025*, 10496–10505.

Tang, F.; Huang, Z.; Liu, C.; Sun, Q.; Yang, H.; and Lim, S. 2025. Intervening Anchor Token: Decoding Strategy in Alleviating Hallucinations for MLLMs. In *The Thirteenth International Conference on Learning Representations, ICLR 2025*.

Touvron, H.; Lavril, T.; Izacard, G.; Martinet, X.; Lachaux, M.; Lacroix, T.; Rozière, B.; Goyal, N.; Hambro, E.; Azhar, F.; Rodriguez, A.; Joulin, A.; Grave, E.; and Lample, G. 2023. LLaMA: Open and Efficient Foundation Language Models. *arXiv preprint arXiv:2302.13971*.

Wang, C.; Chen, X.; Zhang, N.; Tian, B.; Xu, H.; Deng, S.; and Chen, H. 2025. MLLM can see? Dynamic Correction Decoding for Hallucination Mitigation. In *The Thirteenth International Conference on Learning Representations, ICLR 2025*.

Wang, J.; Wang, Y.; Xu, G.; Zhang, J.; Gu, Y.; Jia, H.; Wang, J.; Xu, H.; Yan, M.; Zhang, J.; and Sang, J. 2023. AMBER: An LLM-free Multi-dimensional Benchmark for MLLMs Hallucination Evaluation. *arXiv preprint arXiv:2311.07397*.

Wu, S.; Fei, H.; Pan, L.; Wang, W. Y.; Yan, S.; and Chua, T. 2025. Combating Multimodal LLM Hallucination via Bottom-Up Holistic Reasoning. In *AAAI-25, Sponsored by the Association for the Advancement of Artificial Intelligence*, 8460–8468.

Xie, J.; Gao, Y.; You, L.; Xu, X.; Xu, H.; Kou, Z.; Fu, K.; Qu, Y.; Yang, W.; Guo, J.; Meng, W.; Gao, L.; Yang, H.;

Wang, C.; and Zhang, Y. 2025. Collaboration Wins More: Dual-Modal Collaborative Attention Reinforcement for Mitigating Large Vision Language Models Hallucination. In *Proceedings of the 33rd ACM International Conference on Multimedia, MM 2025*, 4137–4146.

Yang, Z.; Luo, X.; Han, D.; Xu, Y.; and Li, D. 2025. Mitigating Hallucinations in Large Vision-Language Models via DPO: On-Policy Data Hold the Key. In *IEEE/CVF Conference on Computer Vision and Pattern Recognition, CVPR 2025*, 10610–10620.

Yin, S.; Fu, C.; Zhao, S.; Xu, T.; Wang, H.; Sui, D.; Shen, Y.; Li, K.; Sun, X.; and Chen, E. 2024. Woodpecker: hallucination correction for multimodal large language models. *Sci. China Inf. Sci.*, 67(12).

Yin, Y.; Xie, Y.; Yang, W.; Yang, D.; Ru, J.; Zhuang, X.; Liang, L.; and Zou, Y. 2025. ATRI: Mitigating Multilingual Audio Text Retrieval Inconsistencies by Reducing Data Distribution Errors. In *Proceedings of the 63rd Annual Meeting of the Association for Computational Linguistics, ACL 2025, Vienna, Austria, July 27–August 1, 2025*.

Zhang, P.; Su, Y.; Wu, P.; An, D.; Zhang, L.; Wang, Z.; Wang, D.; Ding, Y.; Zhao, B.; and Li, X. 2025a. Cross from Left to Right Brain: Adaptive Text Dreamer for Vision-and-Language Navigation. *arXiv preprint arXiv:2505.20897*.

Zhang, Y.; Xie, R.; Sun, X.; Huang, Y.; Chen, J.; Kang, Z.; Wang, D.; and Wang, Y. 2025b. DHCP: Detecting Hallucinations by Cross-modal Attention Pattern in Large Vision-Language Models. In *Proceedings of the 33rd ACM International Conference on Multimedia, MM 2025*, 3555–3564.

Zhang, Z.; Yadav, S.; Han, F.; and Shutova, E. 2025c. Cross-modal Information Flow in Multimodal Large Language Models. In *IEEE/CVF Conference on Computer Vision and Pattern Recognition, CVPR 2025, Nashville, TN, USA, June 11-15, 2025*, 19781–19791.

Zhao, Q.; Zhang, X.; Li, Y.; Xing, Y.; Yuan, X.; Tang, F.; Fan, S.; Chen, X.; Wang, D.; and Zhang, X. 2025. MCA-LLaVA: Manhattan Causal Attention for Reducing Hallucination in Large Vision-Language Models. In *Proceedings of the 33rd ACM International Conference on Multimedia, MM 2025*, 3981–3990.

Zhuang, X.; Xie, Y.; Deng, Y.; Liang, L.; Ru, J.; Yin, Y.; and Zou, Y. 2025a. VARGPT: Unified Understanding and Generation in a Visual Autoregressive Multimodal Large Language Model. *arXiv preprint arXiv:2501.12327*.

Zhuang, X.; Xie, Y.; Deng, Y.; Yang, D.; Liang, L.; Ru, J.; Yin, Y.; and Zou, Y. 2025b. VARGPT-v1.1: Improve Visual Autoregressive Large Unified Model via Iterative Instruction Tuning and Reinforcement Learning. *arXiv preprint arXiv:2504.02949*.